

# Multidimensional high-resolution NMR structural characterization of a carborane cluster derivative: The case of 2-amino-3-(1,7-dicarba-*closo*-dodecaboranyl-1-thio)propanoic acid

Tianyu He, Rabi A. Musah\*

Department of Chemistry, University at Albany, State University of New York, 1400 Washington Avenue, Albany, NY 12222, USA

## ARTICLE INFO

### Article history:

Received 1 December 2018

Accepted 14 February 2019

Available online 22 February 2019

### Keywords:

NMR spectroscopy

Carborane

Amino acid

Boron

Structural elucidation

## ABSTRACT

Carbon-bearing boron hydrides, also known as carboranes, are polyhedral clusters composed of hydrogen, boron, and carbon and are closely related to boranes. Because of their esthetically pleasing symmetry as well as unusual chemical properties, carboranes have attracted immense interest. Studies over the past 40 years have revealed them to have chemical features that make them useful in a number of specialized applications such as conducting organic polymers, nuclear waste remediation, and as liquid crystalline materials. It has also been shown that carboranes can be used as boron delivery agents for boron neutron capture therapy against cancer. While a number of strides have been made in synthesizing these molecules, their characterization by NMR spectroscopy is challenging due to boron–boron and boron–hydrogen coupling. This gives rise to broad and unresolved peaks and makes peak assignment difficult and often based on best guesses. NMR structural characterization studies of carborane compounds are sparse, dated, and often performed at low resolution. This report provides a detailed structural characterization of an *m*-carborane derivative, featuring high-resolution multi-dimensional NMR spectroscopy (2-D  $^1\text{H}$ – $^1\text{H}$ , 2-D  $^{11}\text{B}$ – $^{11}\text{B}$ , 2-D  $^{11}\text{B}$ – $^1\text{H}$ , and 2-D  $^{13}\text{C}$ – $^1\text{H}$ ). The asymmetry of the carborane cluster (a consequence of substitution at one of the two cluster carbons) adds a dimension of complexity to the spectra, whose peaks could be assigned nevertheless due to their high resolution.

© 2019 Elsevier Ltd. All rights reserved.

## 1. Introduction

Carbon-containing boron cluster compounds, also known as carboranes, are clusters composed of boron, carbon and hydrogen atoms. Like many of the boranes, they are polyhedral and are classified as *closo*-, *nido*-, *arachno*-, *hypho*-, etc., based on whether they represent a complete (*closo*-) polyhedron, or a polyhedron that is missing one (*nido*-), two (*arachno*-), or more vertices. Dicarba-*closo*-dodecaboranes are carboranes that contain two carbons and ten boron atoms that adopt an icosahedral geometry. These icosahedral carboranes ( $\text{C}_2\text{B}_{10}\text{H}_{12}$ ) and their derivatives were first synthesized and characterized in the 1960s [1–4].

One of the most astonishing properties of molecules of the formula  $\text{C}_2\text{B}_{10}\text{H}_{12}$  is that each of the heavy atoms including carbon is hexacoordinated to form the icosahedral cluster. Because of their esthetically pleasing symmetry as well as their unusual chemistry, carboranes and their derivatives have attracted immense interest. Over the past 40 years, a series of B- and C-substituted carboranes

have been prepared, and their synthetic conditions have revealed the remarkable chemical and thermal stability of the icosahedral cage [5]. It has also been shown that they can undergo a variety of organic reactions.

There are two stable isotopes of boron,  $^{10}\text{B}$  and  $^{11}\text{B}$ . Both nuclei are quadrupolar and thus, the boron NMR signal is usually broad ( $>10\text{ Hz}$ ).  $^{11}\text{B}$  is commonly regarded as more suitable for NMR studies because of its higher sensitivity, better resolution at a given external magnetic field, and higher natural abundance (80.4%) [6]. The precise connectivities between the atoms within the carborane cluster can be difficult to establish because of the complexity of their  $^{11}\text{B}$  and  $^1\text{H}$  NMR spectra. Inter- and intramolecular interactions, nuclear relaxation effects, and the limited understanding of the effects of the coupling between borons, as well as that between B and H, which results in broad, overlapping, and unresolved peaks, are the main contributors to this problem. At present, accurate structural characterization of such compounds is mostly dependent on single crystal X-ray crystallography.

Reports of NMR studies of carboranes have been sparse. In 1969, Eaton and Lipcomb concluded that the  $^{11}\text{B}$  NMR spectra of *o*- and *m*-carboranes were not definitive, and that the assignments were

\* Corresponding author.

E-mail address: [rmusah@albany.edu](mailto:rmusah@albany.edu) (R.A. Musah).

often based on best guesses [7]. For *o*- and *m*-carboranes and their derivatives,  $^{11}\text{B}$  NMR spectra have been acquired at 19.3 MHz [8,9], 32.1 MHz [10], 60 MHz [11], and 64.2 MHz [9]. Although peak assignments were made in these studies, some were based on the assumption that the electronegativities of the boron atoms that are adjacent to carbon are greater than those of the boron atoms that are more distant from the carbons. In 1977, Todd et al. reported “high-resolution” (70.6 MHz)  $^1\text{H}$  and  $^{11}\text{B}$  NMR studies of both *m*- and *o*-carboranes [12], and concluded that there was an error in the postulated assignments reported in earlier studies. They also concluded that the  $^1\text{H}$  NMR spectra in earlier studies of *m*-carborane were too poorly resolved for assignments to be made. As a result of the challenges cited above, most recent reports in which carborane and its derivatives have appeared, generally do not provide detailed assignments of the peaks in the  $^1\text{H}$  and  $^{11}\text{B}$  NMR spectra [13–15].

We report here an NMR structure elucidation study of 2-amino-3-(1,7-dicarba-*closo*-dodecaboranyl-1-thio)propanoic acid (ADPA), featuring  $^1\text{H}$ ,  $^1\text{H}$ - $^1\text{H}$ ,  $^{11}\text{B}$ ,  $^{11}\text{B}$ - $^{11}\text{B}$ ,  $^{11}\text{B}$ - $^1\text{H}$  HMQC,  $^{13}\text{C}$ - $^1\text{H}$  HSQC, and  $^{13}\text{C}$ - $^1\text{H}$  HMBC, using 500 MHz NMR spectroscopy. From the results, the various peaks representative of the borons in the cluster could be assigned.

## 2. Material and methods

The  $\alpha$ -amino acid 2-amino-3-(1,7-dicarba-*closo*-dodecaboranyl-1-thio)propanoic acid (ADPA) that was characterized by NMR spectroscopy was synthesized according to a previously established protocol by He et al. [16]. The methanol- $d_4$  used as the NMR solvent was purchased from Sigma Aldrich (St. Louis, MO). NMR spectra were collected using a Bruker 500 MHz AVIIIHD system with a PRODIGY BBO probe installed (Billerica, MA) ( $^{11}\text{B}$ , 160.4 MHz,  $^1\text{H}$ , 500 MHz,  $^{13}\text{C}$ , 125.7 MHz). All spectra were recorded in methanol- $d_4$ . Referencing was to external  $\text{BF}_3\text{O}(\text{CH}_2\text{CH}_3)_2$  for  $^{11}\text{B}$  NMR and tetramethylsilane (TMS) for  $^1\text{H}$  NMR. The spectra were processed using Topspin 3.5 software (Bruker, Inc). For all NMR experiments, the concentration of ADPA was  $\sim 3.8$  mM. The NMR spectra were acquired at room temperature.

### 2.1. One-dimensional (1-D) $^1\text{H}$ NMR spectroscopy with $^{11}\text{B}$ decoupling

The following parameters were used to collect the 1-D  $^1\text{H}$  NMR spectrum of ADPA: recycle delay (d1) = 1.0 s; acquisition time (AQ) = 5.45 s; number of scans (NS) = 16. The spectral window was 11 ppm centered at 5 ppm.

### 2.2. Two-dimensional (2-D) $^{13}\text{C}$ - $^1\text{H}$ NMR spectroscopy

The  $^{13}\text{C}$ - $^1\text{H}$  HSQC experiment was collected using 2048  $t_1$  points and 256  $t_2$  points in  $^1\text{H}$  and  $^{13}\text{C}$  dimensions, respectively [17]. The following parameters were used: recycle delay (d1) = 1.0 s; acquisition time (AQ) = 0.137 s; number of scans (ns) = 4. The spectral windows were 15 ppm in the  $^1\text{H}$  dimension centered at 6.5 ppm and 180 ppm in the  $^{13}\text{C}$  dimension centered at 90 ppm. The spectrum was apodized with squared sine-bell before Fourier transformation.

The  $^{13}\text{C}$ - $^1\text{H}$  HMBC experiment was collected using 4096  $t_1$  points and 256  $t_2$  points in  $^1\text{H}$  and  $^{13}\text{C}$  dimensions, respectively. The following parameters were used: recycle delay (d1) = 1.0 s; acquisition time (AQ) = 0.273 s; number of scans (NS) = 8. The spectral windows were 15 ppm in the  $^1\text{H}$  dimension centered at 6.5 ppm and 190 ppm in the  $^{13}\text{C}$  dimension centered at 90 ppm. The spectrum was apodized with squared sine-bell before Fourier transformation.

### 2.3. Two-dimensional (2-D) $^1\text{H}$ - $^1\text{H}$ NMR spectroscopy

The spectrum was collected using 2048  $t_1$  points and 256  $t_2$  points in  $^1\text{H}$  direct and indirect dimensions, respectively. The following parameters were used: recycle delay (d1) = 1.0 s; acquisition time (AQ): 0.205 s; number of scans (NS) = 4. The spectral windows were 10 ppm in both the  $^1\text{H}$  direct and indirect dimensions centered at 4.8 ppm. The spectrum was apodized with squared sine-bell before Fourier transformation.

### 2.4. One-dimensional (1-D) $^{11}\text{B}$ NMR spectroscopy

The following parameters were used to collect the 1-D  $^{11}\text{B}$  NMR spectrum of ADPA: recycle delay (d1) = 1.0 s; acquisition time (AQ) = 1.28 s; number of scans (NS) = 16.

### 2.5. Two-dimensional (2-D) $^{11}\text{B}$ - $^{11}\text{B}$ NMR spectroscopy with $^1\text{H}$ decoupling

The spectrum was collected using 1024  $t_1$  points and 256  $t_2$  points in  $^{11}\text{B}$  direct and indirect dimensions, respectively. The following parameters were used: recycle delay (d1) = 1.0 s; number of scans (NS) = 2. The spectral windows were 40 ppm in both the  $^{11}\text{B}$  direct and indirect dimensions centered at  $-10$  ppm.  $^{11}\text{B}$ - $^{11}\text{B}$  polarization transfer took place during evolution in the indirect dimension. The first B pulse was  $90^\circ$  and the second B pulse was  $45^\circ$ . Acquisition time (79 ms) was optimized to resolve the peaks in the spectrum. The spectrum was apodized with squared sine-bell before Fourier transformation.

### 2.6. Two-dimensional (2-D) $^1\text{H}$ - $^1\text{H}$ NMR spectroscopy

The COSY experiment was collected using 2048  $t_1$  points and 256  $t_2$  points in the  $^1\text{H}$  direct and indirect dimensions respectively. The following parameters were used to collect the COSY spectrum: recycle delay (d1) = 1.0 s; acquisition time (AQ) = 0.205 s; number of scans (NS) = 4. The spectral windows were 9.6 ppm for both the  $^1\text{H}$  direct and indirect dimensions centered at 4.8 ppm. The spectrum was apodized with squared sine-bell before Fourier transformation.

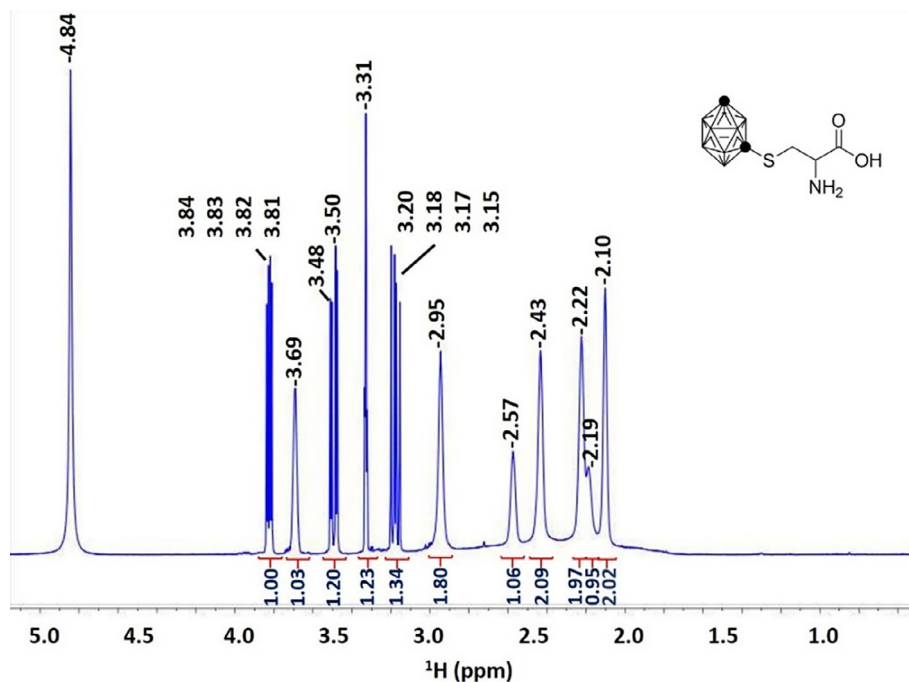
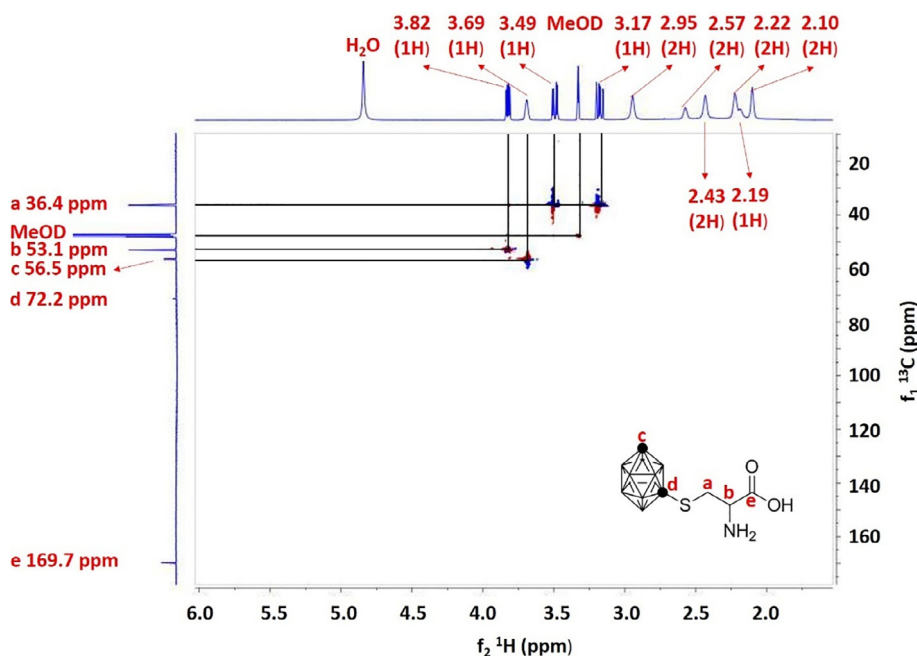
### 2.7. Two-dimensional (2-D) $^{11}\text{B}$ - $^1\text{H}$ NMR spectroscopy

The spectrum was collected using 8192  $t_1$  points and 128  $t_2$  points in the  $^1\text{H}$  and  $^{11}\text{B}$  dimensions respectively. The following parameters were used: recycle delay (d1) = 1.0 s; number of scans (NS) = 4. The spectral windows were 12.8 ppm in the  $^1\text{H}$  dimension centered at 6.5 ppm and 30 ppm in the  $^{11}\text{B}$  dimension centered at  $-10$  ppm. The polarization transfer delay was optimized assuming that  $J_{\text{B-H}} = 150$  Hz. Acquisition time (638 ms) was optimized to resolve the peaks in the spectrum. The spectrum was apodized with squared sine-bell before Fourier transformation.

## 3. Results

### 3.1. 2-D $^{13}\text{C}$ - $^1\text{H}$ (HSQC) and 2-D $^{13}\text{C}$ - $^1\text{H}$ (HMBC) NMR spectroscopy of ADPA

A  $^{11}\text{B}$  decoupled  $^1\text{H}$  spectrum of ADPA was collected (Fig. 1) (labeled with chemical shifts in ppm and integration ratios). In order to assign the H peaks in the  $^{11}\text{B}$  decoupled  $^1\text{H}$  NMR spectrum, 2-D  $^{13}\text{C}$ - $^1\text{H}$  NMR spectra (HSQC and HMBC) were acquired to investigate the correlations. The peaks in the 2-D  $^{13}\text{C}$ - $^1\text{H}$  (HSQC) NMR spectrum (Fig. 2) are labeled a, b, c, d and e, which corresponds to the labels given to the carbons in the structure of ADPA

Fig. 1.  $^{11}\text{B}$  decoupled  $^1\text{H}$  NMR spectrum of ADPA.Fig. 2. 2-D  $^{13}\text{C}$ - $^1\text{H}$  HSQC NMR spectrum of ADPA.

that is shown. In the structure of ADPA, the carbonyl carbon  $\text{C}_e$  and  $\text{C}_d$  within the carborane cluster are not bound to protons and therefore, no cross-peaks are expected for these carbons, as was observed. The two protons of the methylene group adjacent to S are diastereotopic because of the chirality of the  $\alpha$  carbon in the amino acid. These two protons are represented by the two doublets of doublets in the  $^1\text{H}$  NMR spectrum of ADPA, with peaks centered at 3.49 (dd-1H) and 3.17 ppm (dd-1H), due to the splitting of the two protons by each other and by the H on the  $\alpha$  carbon. Hence, two signals are expected for the methylene  $\text{C}_a$ . In the 2-D  $^{13}\text{C}$ - $^1\text{H}$  HSQC NMR spectrum (Fig. 2), the most downfield C peak at

169.7 ppm represents the carbonyl  $\text{C}_e$  for which no proton connectivity was observed. The other C that had no proton connectivity was ascribed to the carborane cluster  $\text{C}_d$  at 72.2 ppm. The peak at 56.5 ppm with a cross-peak intersecting 3.69 ppm (1H) is a result of the second carbon on the carborane cluster  $\text{C}_c$ . Furthermore, the chiral center  $\text{C}_b$  which is connected to one proton resulted in the peak at 53.1 ppm, as a cross-peak intersecting 53.1 and 3.82 ppm was observed. Lastly, the peak at 36.4 ppm which has two cross-peaks intersecting at 3.49 (1H) and 3.17 (1H) ppm corresponds to  $\text{C}_a$ , to which two diastereotopic protons are attached.

To validate the assignments, we obtained the 2-D  $^{13}\text{C}$ – $^1\text{H}$  HMBC NMR spectrum illustrated in Fig. 3. The previously assigned  $\text{C}_e$  at 169.7 ppm has three cross-peaks at 3.82 ppm (1H), 3.49 ppm (1H), and 3.17 ppm (1H) corresponding to a proton on  $\text{C}_b$ , and the two diastereotopic protons on  $\text{C}_a$  respectively. The carborane cluster carbon  $\text{C}_d$  was observed to have two cross-peaks intersecting at 3.49 (1H) and 3.17 ppm (1H), indicating connectivity to  $\text{C}_a$ , while no connectivity was observed for the other carbon within the cluster  $\text{C}_c$ . The diastereotopic nature of the methylene protons was validated by the connectivity observed for  $\text{C}_b$  (53.1 ppm) with cross-peaks at 3.49 and 3.17 ppm. Lastly, the cross-peak at 3.82 ppm is a result of the bonding between  $\text{C}_a$  and  $\text{C}_b$  to which one proton is attached. The interpretation of the peaks from the 2-D  $^{13}\text{C}$ – $^1\text{H}$  HMBC NMR spectrum is consistent with the peak assignments made above.

### 3.2. 2-D $^1\text{H}$ – $^1\text{H}$ (COSY) NMR spectroscopy of ADPA

Since the  $^1\text{H}$  spectrum is better resolved than the  $^{11}\text{B}$  spectrum, a 2-D COSY spectrum was collected to validate the assignments of the protons on the amino acid backbone. In the COSY experiment (Fig. 4), the proton peaks are labeled based on the labels assigned to the carbons to which they are connected ( $\text{H}_a$ ,  $\text{H}_b$ , and  $\text{H}_c$ ). The peak attribution made earlier were confirmed by the cross-peak signals of the two diastereotopic protons  $\text{H}_a$  and  $\text{H}_b$ . The two signals for  $\text{H}_a$  intersect one another and  $\text{H}_b$ , while the  $\text{H}_b$  signal intersects the two signals from  $\text{H}_a$ . As anticipated, no cross-peak signal was observed for  $\text{H}_c$ .

### 3.3. Connectivity of the boron atoms revealed by 2-D $^{11}\text{B}$ – $^1\text{H}$ (HMQC) NMR spectroscopy

Unlike some of the previous carborane structure elucidation studies that featured unsubstituted clusters [9,12], ADPA is distinguished in that the two carbons (1 and 7), which have a *meta* relationship, are not identical. The cysteine-based substituent group that is bound at C (1) allows the two carbons to be distinguished, and the differences between the two carbons would be expected to increase the complexity of the  $^{11}\text{B}$  spectrum, relative to that of the unsubstituted carborane. One way in which to visualize the

coupling relationships between the atoms in the carborane moiety is to view the icosahedron in flattened form, as presented in Fig. 5. Panel A shows the icosahedron in cage form with the atoms labeled according to the conventional numbering system, while Panel B illustrates it in a flattened form, utilizing the same numbering system. In this flattened rendering, it is apparent that the pairs B (2)/(3); B (4)/(6); B (8)/(11); and B (9)/(10) are each equivalent. B (5) and B (12) are each non-equivalent and unique. Thus, six different  $^{11}\text{B}$  signals would be anticipated in the  $^{11}\text{B}$  spectrum. This expectation is borne out by experiment, as illustrated in the broad band decoupled 1-D  $^{11}\text{B}$  NMR spectrum of ADPA shown in Fig. 6. The signals extend from –14.40 to –3.71 ppm, reflecting the electropositive nature of B as compared to carbon. Peak integration for the signals at –3.71 ppm, the cluster extending from –9.24 to –10.57 ppm (centered at –10.17 ppm), and the peaks at –13.8 and –14.0 ppm were 1:5:2:2, accurately indicating that the borons are 10 in number.

In order to account for the remaining protons from the  $^1\text{H}$  NMR spectrum (Fig. 1) that are associated with the carborane cage, a 2-D  $^{11}\text{B}$ – $^1\text{H}$  (HMQC) NMR spectrum was acquired (with preliminary B assignments based on H chemical shifts). The assignments were made based on the well-known influence of the carbon atoms on the relative chemical shifts of the B signals [9]. Carbons (1) and (7) induce a diamagnetic effect which causes the adjacent boron atoms to appear upfield. Thus, the most upfield signal at –14.40 ppm was attributed to B (2)/(3), which are equidistant from, and are the boron atoms that are closest to C (1) and C (7). Farthest from the two carbons is B (5). Consequently, its chemical shift was anticipated to be the most downfield. Therefore, the signal at –3.71 ppm was assigned to B (5). Next to B (2)/(3) in terms of proximity to C (1) and C (7) is the B (8)/(11) pair, to which the signal at –13.18 ppm was attributed. The peak cluster centered at –10.17 ppm was ascribed to the B (4)/(6) and B (9)/(10) pairs, and B (12) based on their proximity to C (1) and C (7) (relative to that of the B (2)/(3) and B (8)/(11) pairs). Among these boron atoms, the B (4)/(6) pair is closer to the two carbons than the B (9)/(10) pair and B (12). Thus, the most upfield peak in the cluster (–10.57 ppm) was assigned to B (4)/(6). Similarly, the farther B (9)/(10) pair was ascribed to the peak at –10.09 ppm, and the unique B (12) was assigned to the peak at –9.24 ppm.

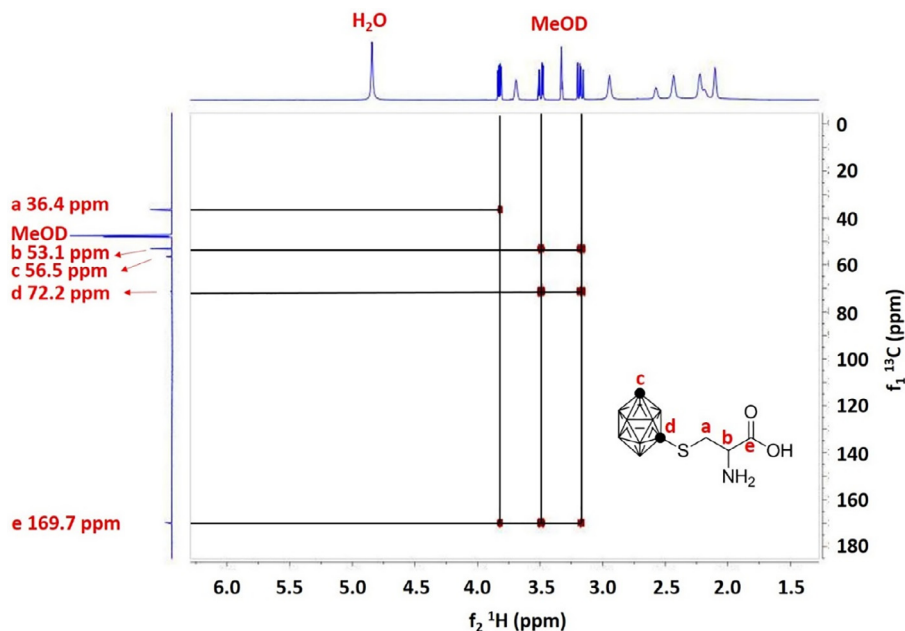


Fig. 3. 2-D  $^{13}\text{C}$ – $^1\text{H}$  HMBC NMR spectrum of ADPA.

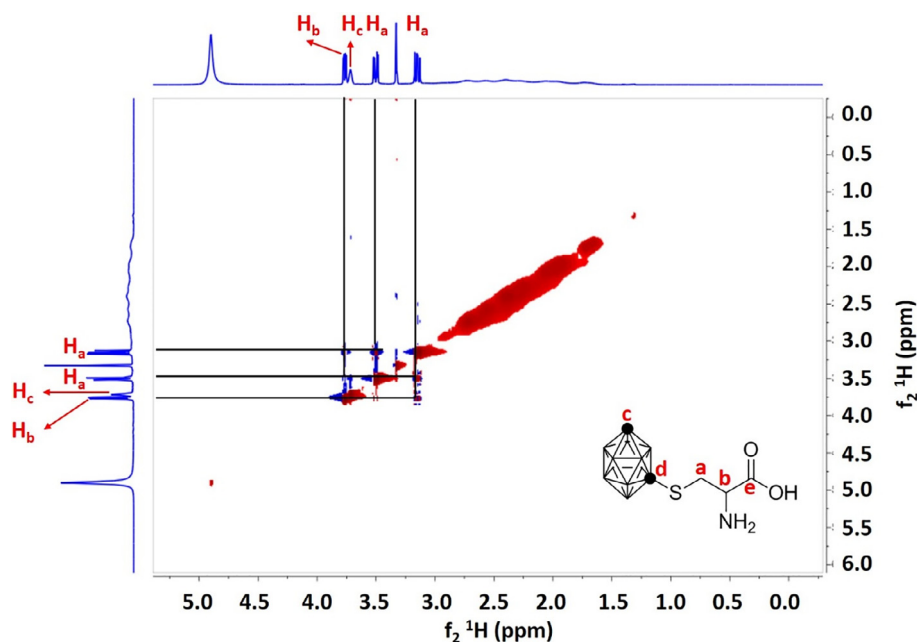


Fig. 4. 2-D  $^{13}\text{C}$ – $^1\text{H}$  HMBC NMR spectrum of ADPA.

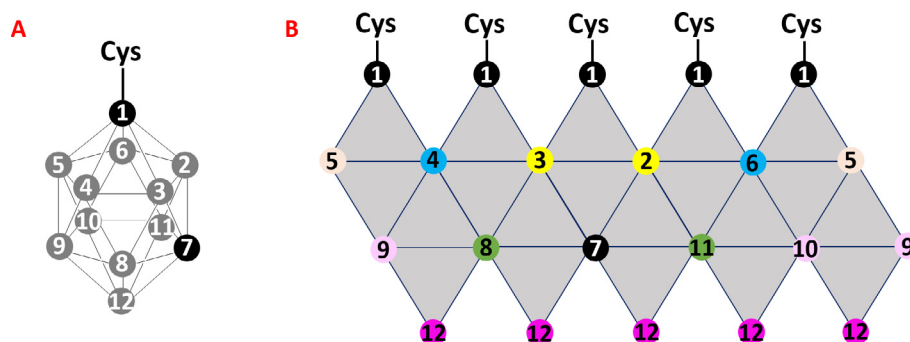


Fig. 5. The icosahedron cage of *m*-carborane numbered according to the conventional system (A) and rendered in its flattened form (B) while retaining the numbering system. Black circles indicate carbons and all other numbered atoms are borons. The boron atoms are color coded to indicate pairs that have equivalent distance to carbon atoms.

It was observed in the 2-D  $^{11}\text{B}$ – $^1\text{H}$  HMQC experiment (Fig. 7) that the cross-peaks are present for all B atoms. The previous assignment of the peak cluster centered at  $-10.17$  ppm in the 1-D  $^{11}\text{B}$  NMR spectrum (Fig. 6) to three different types of B atoms, B (4)/(6), B (9)/(10), and B (12), was confirmed by the connectivity of these B atoms to three types of protons. These three types of protons appeared upfield in the  $^1\text{H}$  NMR spectrum (Fig. 1) with chemical shifts of 2.10 ppm (B (4)/(6)-2H), 2.19 ppm (B (12)-1H), and 2.43 ppm (B (9)/(10)-2H). B (5) is connected to the proton (1H) at 2.57 ppm, and B (8)/(11) and B (2)/(3) are connected to the protons (2H) at 2.22 and 2.95 ppm (2H each), respectively. Of the two pairs, it was anticipated that B (2)-H and B (3)-H would appear further downfield because of the diamagnetic influence of the adjacent C (1) and C (7) atoms.

#### 3.4. Confirmation of assignments by 2-D $^{11}\text{B}$ – $^{11}\text{B}$ (COSY) NMR spectroscopy of ADPA

To confirm the assignments and the connectivities of the B atoms within the cluster, the 2-D  $^{11}\text{B}$ – $^{11}\text{B}$  NMR spectrum shown in Fig. 8 was obtained. The boron that is farthest from C (1) and C (7) (i.e. B (5)) and which is represented by the peak at  $-3.71$  ppm, is bonded to B (4)/(6) and (9)/(10). The cross peaks

which intersect with the signals at  $-3.71$  and  $-10.57$  ppm, and  $-3.71$  and  $-10.09$  ppm confirmed this assignment, which is indicated by the 2-D  $^{11}\text{B}$  NMR spectrum in Fig. 8. As shown by the cross-peaks in Fig. 8, the connectivities of B (12) were confirmed by the cross-peaks which intersect with the signals at  $-9.24$  and  $-10.09$  ppm (connectivity with the B (9)/(10) pair) and  $-9.24$  and  $-13.18$  ppm (connectivity with the B (8)/(11) pair). The pair B (9)/(10) is expected to connect with boron pairs (8)/(11) and (4)/(6), as well as the unique borons (5 and 12). The cross-peaks that intersect at  $-13.18$ ,  $-10.57$ ,  $-3.71$ , and  $-9.24$  ppm are present to confirm this assignment. For the boron pair B (4)/(6), the cross-peaks have intersections at  $-14.40$ ,  $-13.18$ ,  $-10.09$ , and  $-3.71$  ppm, indicating connectivities with B (2)/(3), B (8)/(11), B (9)/(10), and B (5) respectively. Lastly, the connectivity between B (2)/(3) and B (8)/(11) was confirmed by the cross-peaks that intersect at  $-14.40$  and  $-13.18$  ppm.

#### 4. Discussion and conclusion

The structure elucidation study presented here sheds the greatest light to date on interpretation of the  $^{11}\text{B}$  and  $^1\text{H}$  NMR spectra of *m*-carborane derivatives. Although NMR studies of carboranes have been previously reported, the peaks were poorly resolved



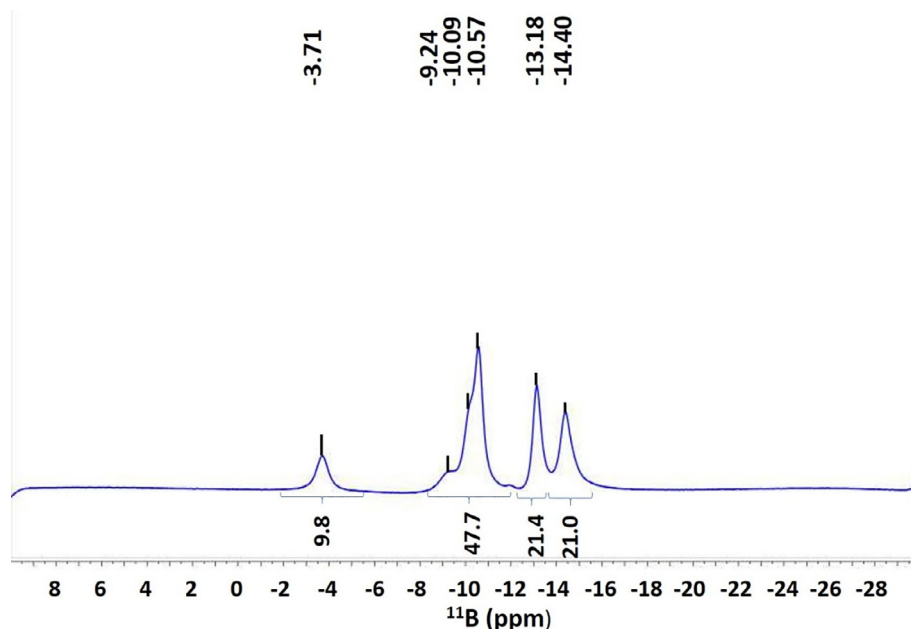


Fig. 6. Broad band decoupled  $^{11}\text{B}$  NMR spectrum of ADPA. (Color online.)

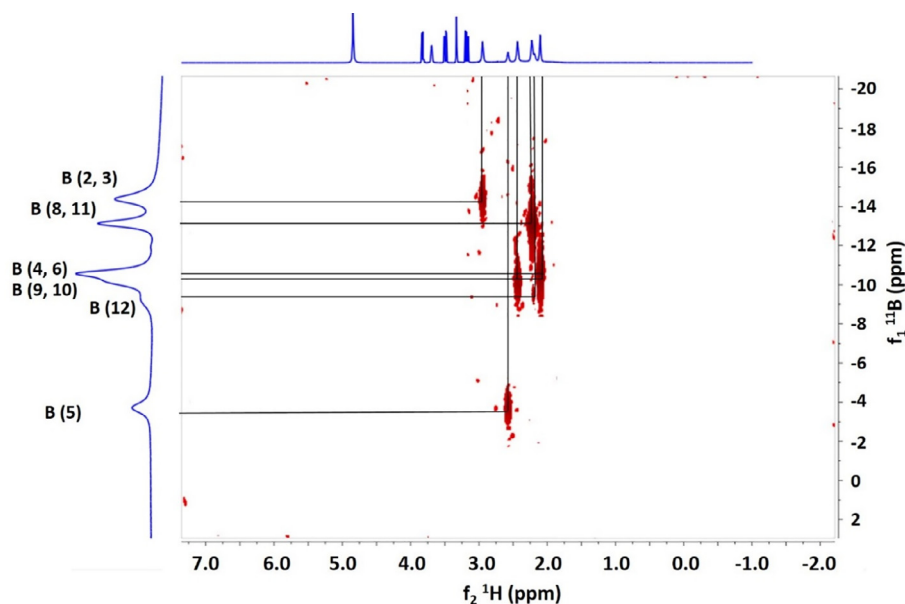


Fig. 7. 2-D  $^{11}\text{B}$ - $^1\text{H}$  HMQC NMR spectrum of ADPA.

because of the low-resolution of the NMR spectra. Furthermore, because of the high degree of symmetry in the unsubstituted carborane molecules in previous reports, the complexity of the spectra were low and thus the reported assignments cannot easily be extended to interpretation of the more complex spectra acquired from unsymmetrical carboranes. Using the flattened icosahedron cage model and paring the 2-D  $^{11}\text{B}$ - $^{11}\text{B}$  NMR spectra with the 1-D  $^{11}\text{B}$  and  $^1\text{H}$  NMR spectra, the proper assignments of both B and H were made more readily apparent. Furthermore, the spectral resolution in this study was greatly enhanced by using a 500 MHz NMR spectrometer, as compared to previous studies.

The 2-D  $^{13}\text{C}$ - $^1\text{H}$  NMR spectra (HSQC and HMQC) demonstrated well-resolved cross-peaks, which provided additional structural

information about the amino acid moiety by illustrating the connectivities within it and enabling differentiation of the diastereotopic protons on the methylene carbon  $\text{C}_\alpha$ . Thus, the work presented here also sheds light on the structural determination by 2-D NMR spectroscopy of amino acids that are associated with carborane and its derivatives, which has not been reported before. Although single crystal X-ray crystallography provides a more certain proof of the structures of carborane and its derivatives, NMR spectroscopy is a more readily applicable method to obtain structural and molecular dynamics information, and can be performed simply and rapidly. Further studies will be focused on expanding the characterization to a variety of carborane clusters, such as *o*- and *p*-carboranes, as well as their derivatives.

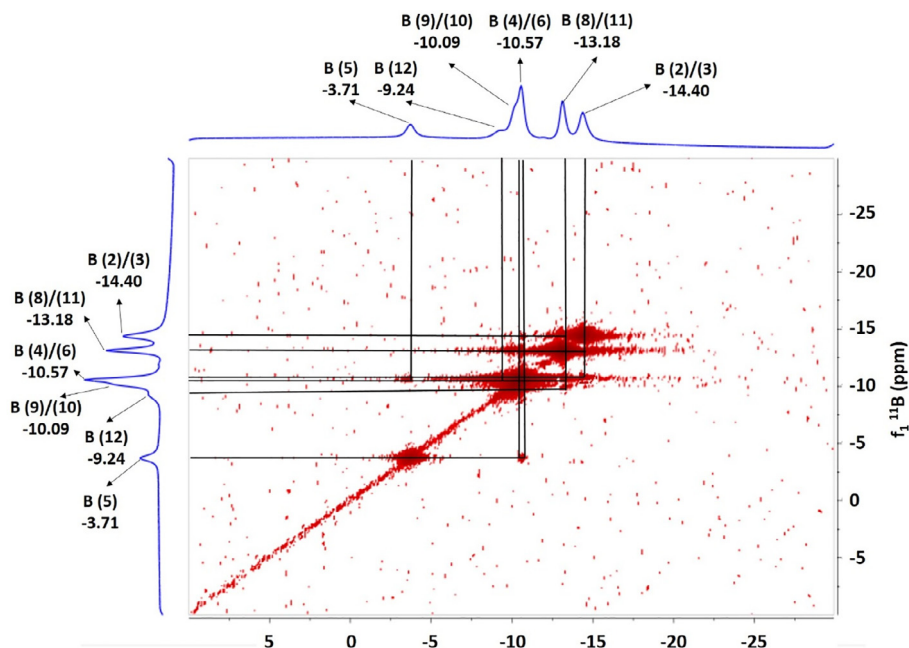


Fig. 8. 2-D  $^{11}\text{B}$ – $^{11}\text{B}$  (COSY) NMR spectrum of ADPA.

## Acknowledgements

Thanks are extended to Prof. Alexander Shekhtman for his assistance with NMR experiments. The financial support of the United States National Science Foundation to R.A.M. (grant 1726724) is gratefully acknowledged.

## References

- [1] M.M. Fein, J. Bobinski, N. Mayes, N. Schwartz, M.S. Cohen, Carboranes. I. The preparation and chemistry of 1-isopropenylcarborane and its derivatives (a new family of stable clovoboranes), *J. Inorg. Chem.* 2 (1963) 1111, <https://doi.org/10.1021/jc50010a007>.
- [2] T.L. Heying et al., A new series of organoboranes. I. Carboranes from the reaction of decaborane with acetylenic compounds, *Inorg. Chem.* 2 (1963) 1089, <https://doi.org/10.1021/jc50010a002>.
- [3] L.I. Zakharkin, V.I. Stanko, V.A. Brattsev, Y.A. Chapovskii, O.Y. Okhlobystin, Synthesis of a new class of organoboron compounds,  $\text{B}_{10}\text{C}_2\text{H}_{12}$  (barene) and its derivatives, *Izv. Akad. Nauk. SSSR, Ser. Khim.* (1963) 2238.
- [4] L.I. Zakharkin, V.I. Stanko, V.A. Brattsev, Y.A. Chapovsky, Y.T. Struchkov, Structure of  $\text{B}_{10}\text{C}_2\text{H}_{12}$  (barene) and its derivatives, *Izv. Akad. Nauk. SSSR, Ser. Khim.* (1963) 2069.
- [5] V.I. Bregadze, Dicarba-closo-dodecaboranes  $\text{C}_2\text{B}_{10}\text{H}_{12}$  and their derivatives, *Chem. Rev.* 92 (1992) 209, <https://doi.org/10.1021/cr00010a002>.
- [6] G.R. Eaton, NMR of boron compounds, *J. Chem. Ed.* 46 (1969) 547, <https://doi.org/10.1021/ed046p547>.
- [7] W. Lipscomb, G. Eaton, *NMR Studies of Boron Hydrides and Related Compounds*, W.A. Benjamin, INC, 1969, pp. 368–386.
- [8] J.A. Potenza, W.N. Lipscomb, G.D. Vickers, H. Schroeder, Order of electrophilic substitution in 1,2-dicarba-closo-dodecaborane(12) and nuclear magnetic resonance assignment, *J. Am. Chem. Soc.* 88 (1966) 628, <https://doi.org/10.1021/ja00955a059>.
- [9] G.D. Vickers, H. Agahigian, E.A. Pier, H. Schroeder, Elucidation of boron ( $^{11}\text{B}$ ) nuclear magnetic resonance spectra by heteronuclear spin decoupling, *J. Inorg. Chem.* 5 (1966) 693, <https://doi.org/10.1021/jc50038a045>.
- [10] V.I. Stanko, V.V. Khrapov, A.I. Klimova, J.N. Shoolery, NMR spectroscopy of carboranes and their derivatives. II. Boron-11 heteronuclear magnetic resonance spectra at 32.08 MHz of *o*- and *m*-carboranes and their dihalo derivatives, *Zh. Strukt. Khim.* 11 (1970) 627.
- [11] R. Pilling, F. Tebbe, M. Hawthorne, E. Pier, Boron-11 nuclear magnetic resonance spectra of two boron hydride derivatives at 60 Mc, *Proc. Chem. Soc., London* (1964) 402.
- [12] A.R. Garber, G.M. Bodner, L.J. Todd, A.R. Siedle, High-resolution  $^1\text{H}$  and  $^{11}\text{B}$  NMR studies of 1,2- and 1,7- $\text{B}_{10}\text{C}_2\text{H}_{12}$ , *J. Magn. Reson.* (1977) 383.
- [13] B.J. Eleazer, M.D. Smith, A.A. Popov, D.V. Peryshkov, (BB)-Carboryne complex of ruthenium: synthesis by double B–H activation at a single metal center, *J. Am. Chem. Soc.* 138 (2016) 10531, <https://doi.org/10.1021/jacs.6b05172>.
- [14] B.A. Izmaylov, V.A. Vasnev, G.D. Markova, On the reactions of haloidmagnesiummethyl-*m*-carboranes with organoalkoxysilanes and chlorosilanes, *Inorg. Chim. Acta* 471 (2018) 475, <https://doi.org/10.1016/j.ica.2017.11.056>.
- [15] A.M. Spokoyny et al., A coordination chemistry dichotomy for icosahedral carborane-based ligands, *Nat. Chem.* 3 (2011) 590, <https://doi.org/10.1038/nchem.1088>.
- [16] T. He, J.C. Misuraca, R.A. Musah, “Carboranyl-cysteine”—Synthesis, structure and self-assembly behavior of a novel  $\alpha$ -amino acid, *Sci. Rep.* 7 (2017) 16995, <https://doi.org/10.1038/s41598-017-16926-w>.
- [17] J. Cavanagh, W.J. Fairbrother, A.G. Palmer, N.J. Skelton, M. Rance, *Protein NMR Spectroscopy Principles and Practice*, Academic Press, 2006.